Article

The Role of Mitochondria in the Dual Effect of Low-Temperature Plasma on Human Bone Marrow Stem Cells: From Apoptosis to Activation of Cell Proliferation

Sergej V. Belov [1], Yakov P. Lobachevsky [2], Yurij K. Danilejko [1], Aleksej B. Egorov [1], Alexander V. Simakin [1], Alireza Maleki [3,4], Andrey A. Temnov [5], Mikhail V. Dubinin [6,*] and Sergey V. Gudkov [1]

[1] Prokhorov General Physics Institute of the Russian Academy of Sciences, Vavilov st. 38, 119991 Moscow, Russia; ser79841825@yandex.ru (S.V.B.); dyuk42@list.ru (Y.K.D.); a261@rambler.ru (A.B.E.); avsimakin@gmail.com (A.V.S.); s_makariy@rambler.ru (S.V.G.)

[2] Federal State Budgetary Scientific Institution "Federal Scientific Agroengineering Center VIM" (FSAC VIM), 1st Institutskiy pr-d 5, 109428 Moscow, Russia; lobachevsky@yandex.ru

[3] Institute of Molecular Medicine, Sechenov University, Bolshaya Pirogovskaya st., 2, 119435 Moscow, Russia; alireza.maleki@mq.edu.au

[4] Department of Physics and Astronomy, Macquarie University, Balaclava Rd, Macquarie Park, Sydney, NSW 2109, Australia

[5] Moscow Institute of Physics and Technology, Institutskaya st. 9, Dolgoprudny, 141701 Moscow, Russia; aa-temnov@yandex.ru

[6] Department of Biochemistry, Cell Biology and Microbiology, Mari State University, pl. Lenina 1, Yoshkar-Ola, 424001 Mari El, Russia

* Correspondence: dubinin1989@gmail.com; Tel.: +79-877-010-437

Abstract: The potential use of low-temperature plasma (LTP) for therapeutic purposes has aroused the concern of many researchers. This paper examines the effect of LTP on the morphofunctional state of human bone marrow stem cells (BMSC). It has been established that LTP-induced oxidative stress has a dual effect on the state of stem cells. On the one hand, a cell culture exposed to LTP exhibits the progression of a destructive processes, which is manifested by the perturbation of the cell's morphology, the initiation of lipid peroxidation and the accumulation of products of this process, like diene conjugates and malondialdehyde, as well as the induction of mitochondrial dysfunction, leading to cell death. On the other hand, the effect of LTP on BMSC located at a distance from the plasma is accompanied by the activation of proliferative processes, as evidenced by the tendency of the activity of mitochondrial biogenesis and fission/fusion processes to increase. The paper discusses the role of mitochondria and reactive oxygen species (ROS) in the cellular response to LTP.

1. Introduction

The creation of highly selective drugs is inevitably accompanied by concomitant side effects. The most common manifestation of such effects is the body's immune response, which includes overreaction of the immune system and individual intolerance to the drug. Therefore, much attention is currently being paid to the search for new methods of non-drug treatment of pathological processes.

In particular, a significant number of studies are aimed at studying the effects of physical factors on the reparative and regenerative properties of biological objects.

Physical factors primarily affect the molecular level of the organization of living organisms, which subsequently leads to changes on the cellular and tissue levels. One of the promising physical factors is low-temperature plasma (LTP). LTP is a stream of partially ionized gas with a temperature close to the ambient value [1,2]. The biological effect of LTP is based on the synergy of strong electric fields and electromagnetic radiation [1,2]. In this case, the effects of these factors lead to the generation of reactive oxygen species (hydroxyl radical, superoxide anion radical, hydrogen peroxide and ozone) and reactive nitrogen species (nitrogen oxide radicals, nitrate and nitrite anions, peroxynitrite and nitric, nitrous and peroxynitrous acids) [3,4], directly affecting the properties of the tissues and cells of living organisms.

Currently, LTP is used in various fields, such as agriculture, the food industry, bioengineering, the purification of exhaust gases, soil and wastewater [5,6]. Plasma reactors working with targets in humid or wet environments are of great importance for biotechnology and medicine. LTP is actively used for antimicrobial and antifungal treatment [7–10]. There is evidence of the use of LTP to control bleeding, which can be used for the effective healing of wounds and burns [11,12], as well as for the tasks of regenerative medicine. LTP is used to increase the biocompatibility of materials and improve drug delivery efficiency [13–15]. It has been shown that LTP can be used in the treatment of neoplasms. In particular, in remarkable articles, the possibility of selective cytotoxic effects from low-temperature plasma in relation to different types of human cells was reported, which made it possible to select the conditions that ensured the selective death of tumor cells [16–18]. It was established that the effect of LTP on tumor cells led to inhibition of the cell cycle and the transition of these cells to different cell death variants [19]. On the other hand, depending on the conditions and time of exposure, LTP is able to stimulate the differentiation of various types of cells (e.g., preosteoblasts, fibroblasts, immune and stem cells) [20–23]. Indeed, much is known about the final effects of LTP on cells and tissues. At the same time, data on the molecular mechanisms underlying them are often scarce and contradictory. However, one could assume that these effects of LTP may be associated with the ROS-induced initiation of intracellular signaling cascades involving subcellular organelles (first of all, mitochondria), which play a crucial role in cell differentiation and proliferation processes, but also, on the other hand, trigger the mechanisms of cell death [24].

The aim of this work was to identify the effect of low-temperature plasma generated by a high-frequency glow discharge in water vapor on the viability and proliferative activity of human bone marrow stem cells (BMSC) and to estimate the role of mitochondria in the cellular response. We have shown that LTP induces a variety of effects on mammalian cells, ranging from mitochondrial degradation and apoptosis due to the overproduction of hydrogen peroxide and lipid peroxidation to increased mitochondrial biogenesis and dynamics of the organelles, reflecting the tendency for increased cell proliferation due to the ROS-induced activation of the fibroblast growth factor (FGFb).

2. Materials and Methods

2.1. Isolation and Cultivation of Human BMSC

Male and female patients older than 18 years of age who were scheduled for non-emergency open heart surgery gave informed consent for participation in the study. Sternal bone marrow was harvested the day of the surgery under general anesthesia. Each patient's chest skin was incised at the midline, and a syringe with an 18-gauge needle containing 5 mL of 10% heparin solution was advanced slowly through the periosteum of the sternum and rotated as it passed through the anterior table. The solution was injected into the sternum and the plunger was pulled back to aspirate 0.015–0.030 L of bone marrow fluid from the sternum. The syringe containing the bone marrow was placed on ice and transported into the laboratory, where the cells were separated. The BMSC were collected by standard density gradient centrifugation with Lympholyte-H. These cells were cultured on Petri dishes

(140 mm) in a MesenCult basal medium containing mesenchymal stem cell stimulator supplements (StemCell Technologies, Kent, WA, USA). The Petri dishes with the cultured cells were placed in a CO_2 incubator at 37 °C in an atmosphere with 5% CO_2 and 95% humidity. After 48 h, the nonadherent cells were removed, and a fresh medium was added to the cells. The medium was changed every 5 days until a monolayer of cells (3×10^3 cells/mL) was obtained. The morphological state of the cells before and after LTP treatment was analyzed using an inverted microscope.

All procedures performed in studies involving human participants were in accordance with the ethical standards of the institutional or national research committee and with the 1964 Helsinki Declaration and its later amendments or comparable ethical standards. The study was approved by the Bioethics Committee of the Sklifosovsky Research Institute of Emergency Medicine (No. 2018/03/21-2).

2.2. The Effects of LTP on Cells

After obtaining a monolayer, the cells were treated with LTP. The schematic diagram of the experimental setup is shown in Figure 1. In this case, a MesenCult basal medium was replaced by Ringer's solution (8.6 g/L NaCl, 0.33 g/L $CaCl_2$ and 0.3 g/L KCl). This was due to the fact that plasma causes local denaturation of the proteins that make up mesenchymal stem cell stimulator supplements, preventing the effects of LTP on BMSC. After the cells were treated with LTP, Ringer's solution was again replaced with a nutrient medium. During the experiment, two electrodes were introduced into the solution layer with a thickness of 6 mm; one needle electrode had a plasma generate on it, while the other annular electrode was neutral. A needle electrode (platinum, 5 mm long, 0.3 mm in diameter and a needle tip diameter of about 50 μm) was inserted into the 3 mm culture solution at an angle of 60° relative to the plane of the cell's monolayer (or at an angle of 30° relative to the axis perpendicular to the plane of the cell's monolayer). An annular neutral electrode (platinum, 0.8 mm in diameter) was installed parallel to the plane of the cell's monolayer, close to the surface of the culture solution. The anode and cathode of the electrode were connected to a high-frequency generator. An impulse voltage of 245 V was applied to the electrode at a 2.64 MHz frequency for 3 s. The appearance of a glow discharge on the electrode surface was detected by a decrease of current flowing through the electrode from 1.8 A to 0.1 A. The resulting discharge was close to an anomalous glow discharge in terms of its physical characteristics [25]. The temperature of the electron gas was close to 5 eV, and the electron concentration was $2-3 \times 10^{18}$ m^{-3}. Ionization in a plasma-forming gas, which is water vapor, is supported mainly by two reactions. Both reactions result in the dissociation of water molecules; one happens through dissociative adhesion, and the other occurs through the excitation of the vibrational degrees of freedom [26]. One should keep in mind that the actual regimen of plasma generation found in the current work (frequencies around 2.6–2.7 MHz) was unique because the elevation of the frequency broke the symmetry of the glowing plasma, making it glow only at one phase, and lift-offs occurred constantly. At the same time, the decrease of the frequency led to non-stationary plasma glowing, and serious fluctuations were observed.
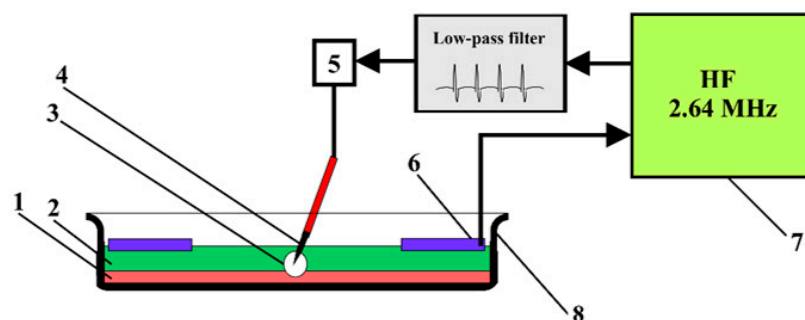

Figure 1. Schematic diagram of the experimental setup, showing (1) the stem cell culture, (2) layer of Ringer's solution, (3) plasma discharge, (4) electrode applicator with a needle, (5) dispenser, (6) ring neutral electrode, (7) high-frequency generator and (8) Petri dish.

2.3. Cell Culture Imaging

The cells were incubated with the following fluorescent markers: 2 μg/mL Hoechst 33342 (Sigma-Aldrich, St. Louis, MO, USA), 2 μg/mL propidium iodide (Sigma-Aldrich, St. Louis, MO, USA) and 0.3 nM mitoTracker Deep Red FM. The propidium iodide dye penetrated into living cells extremely slowly during the short incubation time we used (about 10 min at 37 °C in the dark). It stained only the cells with damaged plasma membranes. The plasma membrane, which had tears through which the dye penetrated, was one of the main signs that the cell was dead. Thus, the Hoechst 33342 marker stained both living and dead cells, while propidium iodide only stained dead cells. The MitoTracker Deep Red FM dye stained all living mitochondria. After staining, the cells were washed from the dyes in Hank's solution for 10 min. Microscopic analysis of the samples was carried out using an image system based on the Leica DMI6000 (Leica Microsystems, Wetzlar, Germany).

2.4. Measurement of Concentration of Hydrogen Peroxide

The concentration of hydrogen peroxide was measured by the chemiluminescence method in a luminol-4-iodinephenol-peroxidase system. The chemiluminescence was measured with the help of a highly sensitive lumenmeter of Biotoks 7 AM (Ekon, Moscow, Russia). The experimental details of the method were described earlier [27].

2.5. Determination of Lipid Peroxidation Products

Lipid peroxidation in the BMSC was estimated spectrophotometrically by measuring the levels of the diene conjugates (DC) and thiobarbituric acid-reactive substances (TBARS). The content of DC in the sample was calculated based on the extinction value at 233 nm for the DC of the polyunsaturated fatty acids equal to 2.2×10^{-5} M^{-1} cm^{-1} [28]. The TBARS assay quantified the levels of malondialdehyde (MDA) via its reaction with thiobarbituric acid. The concentration of TBARS was calculated using the molar absorption coefficient of the colored TBA–MDA complex ($E_{535} = 1.56 \times 10^5$ M$^{-1}\cdot$cm^{-1}) [29].

2.6. Estimation of Mitochondrial Membrane Potential

The mitochondrial membrane potential (MMP) was assessed by the retention of Rhodamine 123 (Rh-123), a specific fluorescent cationic dye that is readily sequestered by active mitochondria, depending on their transmembrane potential [30]. In this case, samples (10^7 cells) were incubated with 6 μM of Rh-123 for 30 min at 37 °C in the dark, then analyzed in a Jasco FP 8300 spectrofluorometer (Halifax, NS, Canada) using an excitation and emission wavelength of 488 nm and 530 nm, respectively.

2.7. RNA Extraction, Reverse Transcription and Quantitative Real-Time PCR

The total RNA was isolated using an ExtractRNA kit (Cat. No. BC032, Eurogen, Moscow, Russia) in accordance with the protocol of the manufacturer. The resulting RNA preparation was treated with RNAse-free DNAse I (Thermo Scientific, Waltham, MA, USA). The concentration of total RNA was measured spectrophotometrically using a Nanodrop ND-1000 spectrophotometer (ND Technologies, Wilmington, DE, USA). Taken for cDNA synthesis was 2 μg of the total RNA. Reverse transcription was performed using an oligo(dT)15 primer and MMLV reverse transcriptase (Eurogen, Moscow, Russia) according to the manufacturer's instructions. Real-time PCR was performed with a DTLite5 amplifier (DNA-Technology LLC, Moscow, Russia) using the qPCRmix-HS SYBR reaction mixture (Eurogen, Moscow, Russia). The selection and analysis of gene-specific primers were performed using Primer-BLAST [31] (the oligonucleotide sequences are presented below in Table 1). The level of gene expression was normalized to β-actin, and a comparative C_T method was used to quantify the results [32].

Table 1. Human-specific primer sequences for quantitative real-time polymerase chain reaction (qRT-PCR).

Gene	Forward (5′ → 3′)	Reverse (5′ → 3′)
Nd1 (mtDNA)	CGCCATAAAACTCTTCACCAAAG	GGGTTCATAGTAGAAGAGCGATGG
Globulin (nDNA)	GTGCACCTGACTCCTGAGGAGA	CCTTGATACCAACCTGCCCAG
β-actin	ACCGAGCGCGGCTACAGC	CTCATTGCCAATGGTGAT
Pink-1	GGGGAGTATGGAGCAGTCAC	CATCAGGGTAGTCGACCAGG
Parkin	TACGTGCACAGACGTCAGGAG	GACAGCCAGCCACACAAGGC
PGC-1α	GTCACCACCCAAATCCTTAT	ATCTACTGCCTGGAGACCTT
Drp1	AGGTTGCCCGTGACAAATGA	ATCAGCAAAGTCGGGGTGTT
Fis1	GTCCAAGAGCACGCAGTTTG	ATGCCTTTACGGATGTCATCATT
Mfn1	ATGACCTGGTGTTAGTAGACAGT	AGACATCAGCATCTAGGCAAAAC
Mfn2	TGATGGGCTACAATGACCAG	AGCTTCTCGCTGGCATGC
Ppif	GACAGACTGGCTAGATGGCAA	CTTCCCACTTTTTGAGCCGA
Opa1	AGCCTCGCAATTTTTGG	AGCCGATCCTAGTATGAGATAGC
Caspase3	GTAGATGGTTTGAGCCTGAG	CCAGTGCGTATGGAGAAATG
JNK	TCCCCCAGCTATCTATATGCAAT	TCACAGCACATGCCACTTGA
SOD1	TTGAACAAGAATCCGAATCC	AGCCAATGACACCACAAGCAG
SOD2	CAGGCAGCTGGCTCCGGTTT	TGCAGTGGATCCTGATTTGG
GPX1	TCCAGACCATTGACATCGAG	ACTGGGATCAACAGGACCAG

2.8. Quantification of Mitochondrial DNA

The total DNA (nuclear and mitochondrial DNA, 10 μg) was extracted from the BMSC using a DNA-Extran 2 kit (Cat. No. EX-511, Sintol, Russia) according to the manufacturer's protocol. For the reaction, 1 ng of the total DNA was taken. Evaluation of the mtDNA content in the samples was performed by PCR, as described in [33], and expressed as an mtDNA/nuclear DNA ratio. For our assay, we selected the ND1 gene of the human mitochondrial genome and globulin, which is a nuclear-encoded gene. A comparison of ND1 DNA expression relative to globulin DNA expression would give a measure of the ratio of the mtDNA copy number to the nDNA copy number. The primers for the mtDNA and nDNA are presented in Table 1. Real-time PCR was performed with a DTLite5 amplifier (DNA-Technology LLC, Moscow, Russia) using the qPCRmix-HS SYBR reaction mixture (Eurogen, Moscow, Russia), containing a commonly used fluorescent DNA binding dye, SYBR Green II.

2.9. FGFb Concentrations Measurement

FGFb concentrations were measured through an enzyme-linked immunosorbent assay (ELISA) using an ELISA commercial kit (RapidBio, West Hills, CA, USA) strictly under the manufacturer's protocol.

2.10. Statistical Analysis

The data were analyzed using GraphPad Prism version 8.0 software for Windows (GraphPad Software, San Diego, CA, USA) and were presented as means ± SEM for three to six experiments (samples from independent donors). All the results were normalized against cell numbers in the corresponding cell culture dishes. Statistical differences between the means were determined by a Mann–Whitney U test, where $p < 0.05$ was considered to be statistically significant.

3. Results

3.1. Hydrogen Peroxide Generation and Lipid Peroxidation (LPO) Induction in BMSC Culture by LTP

At the first stage, we studied the effect of LTP on the formation of reactive oxygen species in the incubation medium. Hydrogen peroxide is the most long-lived ROS form; therefore, we estimated the concentration of this compound. One can see from Figure 2A that LTP induced a dramatic increase in the concentration of hydrogen peroxide in the medium within 1 h after exposure (760-fold). Over the next 48 h, the concentration of hydrogen peroxide decreased by an order of magnitude. After 72 h, the concentration of hydrogen peroxide decreased to the control level. It is known that the overproduction of ROS stimulates oxidation processes, including lipid peroxidation, which is accompanied by the destruction of cell membranes and the damaging of macromolecules [34]. The LTP effects were also found to be accompanied by significant stimulation of the formation of lipid peroxidation products (diene conjugates and malondialdehyde). Within an hour after treatment, the concentration of LPO products increased by three times on average. Moreover, an increased concentration of LPO products was observed for another 48 h. By 72 h of incubation, the concentration of LPO products decreased to the control level (Figure 2B,C).
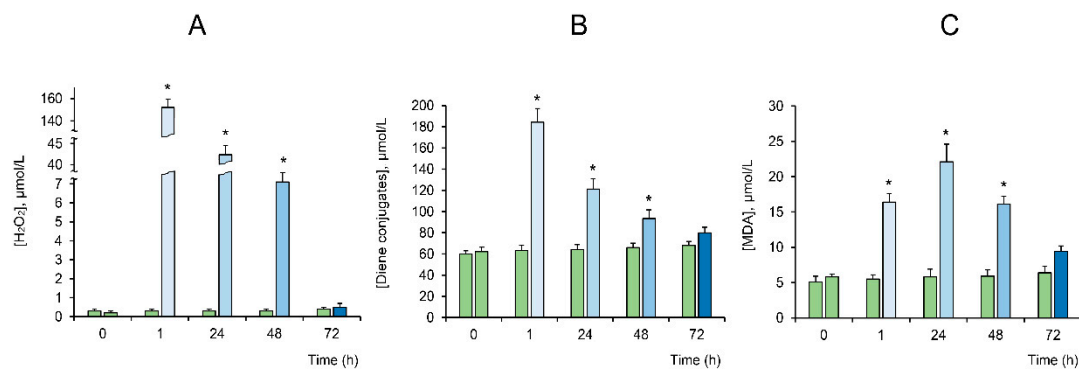

Figure 2. The effect of low-temperature plasma (LTP) on the generation of H_2O_2 in the culture medium (**A**), the content of diene conjugates (DC) (**B**) and malondialdehyde (MDA) (**C**) in the bone marrow stem cells (BMSC) culture (blue bars). The green bars indicate no exposure to plasma (i.e., the control). The values are given as means ± SEM (*n* = 6). * *p* < 0.05 compared to the control.

3.2. Impact of LTP on Mitochondrial Integrity, Biogenesis and Dynamics

It is known that the LPO process, as well as oxidative stress in general, is closely related to the initiation of the selective destruction of mitochondria [35,36]. Indeed, one can see that the BMSC showed a significant decrease in mitochondrial potential during the first 24 h after LTP exposure (Figure 3A). It was accompanied by a decrease in the level of mitochondrial DNA, the inhibition of mitochondrial biogenesis (decrease in PGC-1a expression), fission (decrease in DRP1 expression) and fusion (decrease in OPA1, MFN1 and MFN2 expression) (Figure 3B–G). These processes correlated (R^2 = 0.98) with an increase in the expression level of PTEN-induced putative kinase 1 (PINK1) and the E3 ubiquitin ligase Parkin (PINK1/Parkin, shown in Figure 3H,I), as well as an increase in FIS1 expression, which is typical for mitochondrial degradation and accompanies mitophagy [36–38] (Figure 3J). One can see that, by the 48 h mark of incubation, the membrane potential of the organelles was restored, which was accompanied by the normalization of the level of mtDNA, PGC-1a and organelle fission (DRP1) and fusion (OPA1, MFN1 and MFN2) proteins, as well as a decrease in the expression of PINK1/Parkin to the control levels. Moreover, after 72 h of BMSC incubation, there was a significant increase in the level of mtDNA, the intensity of organelle biogenesis (an increase in PGC-1a) and their fusion processes (increase in OPA1, MFN1 and MFN2) compared with the initial levels of untreated cells. The expression of FIS1 deserves special attention. One can see that the expression of this multifunctional factor was involved in the fission of organelles and, in their degradation [36,38],

simultaneously increased over time significantly. It should be noted that the addition of hydrogen peroxide at concentrations generated by LTP treatment (50–100 μM) did not significantly affect the mitochondrial potential of the BMSC throughout the experiment (Figure 3K,L).
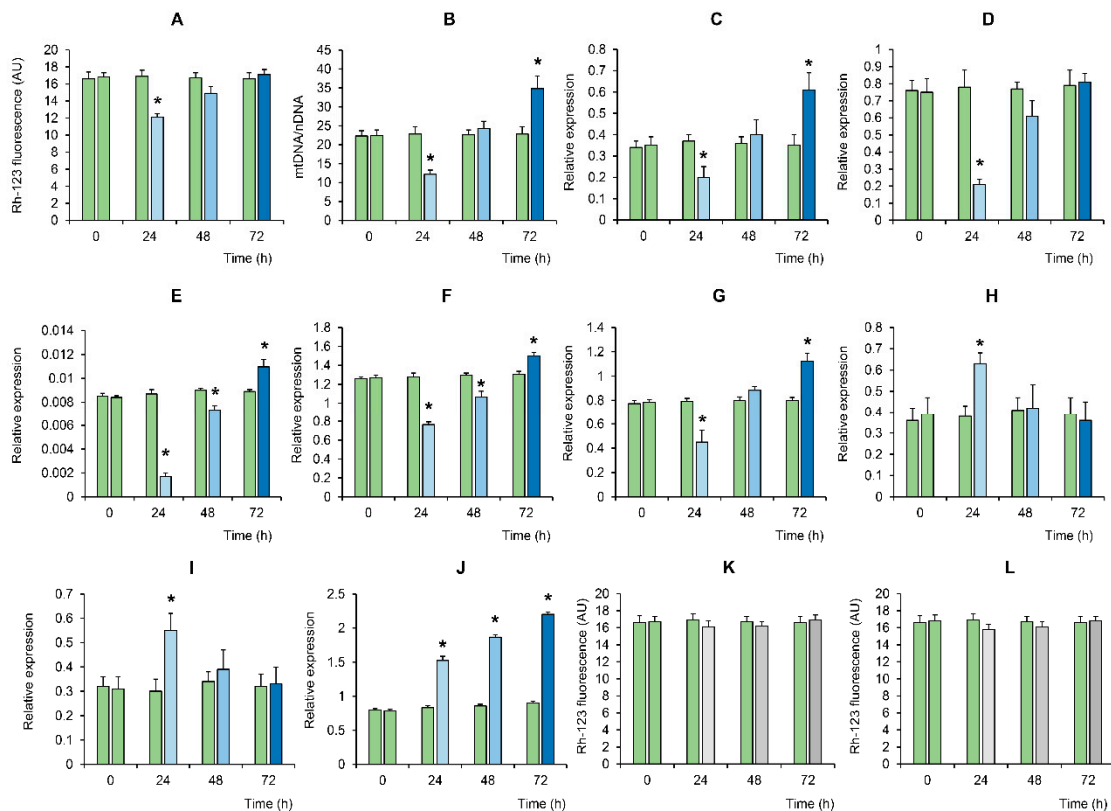

Figure 3. Time-dependent changes in mitochondrial potential, biogenesis and dynamics in the BMSC in response to LTP treatment (blue bars). Panels A and B show the effect of LTP on (**A**) the mitochondrial potential of BMSC, assessed by rhodamine-123 (Rh-123) fluorescence, and (**B**) the ratio of mtDNA to nDNA. A real-time quantitative polymerase chain reaction (qPCR) was carried out to determine the mtDNA copy numbers as a mitochondrial (ND1) to nuclear (globulin) ratio. Panels C–J show the effect of LTP on the relative expression (to β-actin (bAct) of the following genes: (**C**) PGC-1a; (**D**) DRP1; (**E**) OPA1; (**F**) MFN1; (**G**) MFN2; (**H**) PINK1; (**I**) Parkin; and (**J**) FIS1. Panels (**L,K**) show the effect of hydrogen peroxide (50 and 100 μM, respectively) on the mitochondrial potential of the BMSC in the absence of LTP treatment (grey bars). The green bars indicate no exposure to plasma. The values are given as means ± SEM ($n = 3$). * $p < 0.05$ compared to the control.

3.3. Effect of LTP on Cell Death and on the Proliferation and Growth of BMSC

Mitochondrial degradation is known to be closely related to the induction of cell death [36]. We performed a microscopic study on the effect of LTP on the state of a BMSC culture near a needle electrode. One can see that within an hour after exposure of the cell culture to LTP, the cells on the border of the LTP-exposed zone (around 2 mm from the needle electrode) displayed morphological changes specific for the development of apoptosis (e.g., cell shrinkage and fragmentation associated with the formation of apoptotic bodies with compacted chromatin (Figure 4B)). No changes in the morphology of cells located farther from the needle electrode were observed (data not shown).
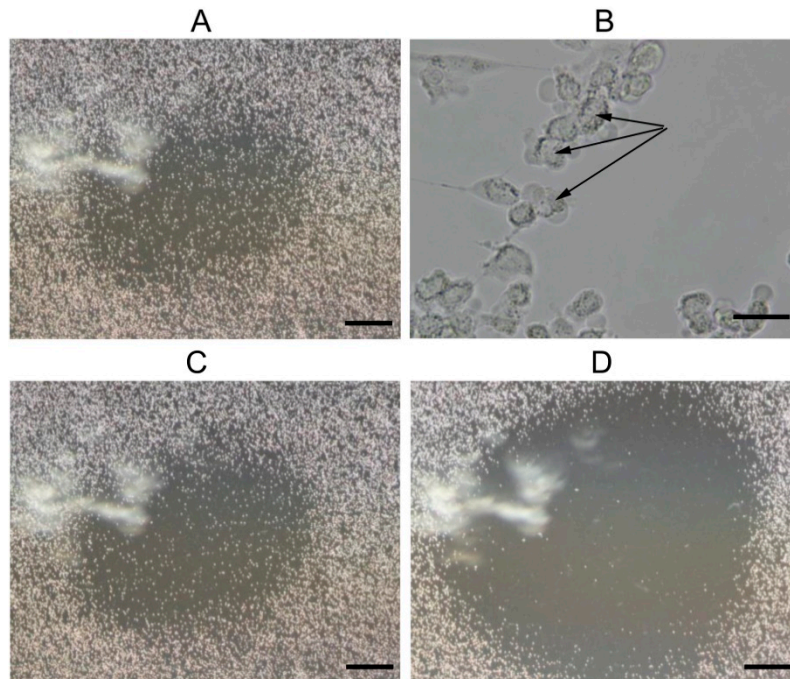
Figure 4. Micrographs of a BMSC culture 1 (**A**,**B**), 24 (**C**) and 36 (**D**) hours after exposure to LTP. Microphotographs were taken at the location of the needle electrode, on which the plasma formation process took place. The scale bars were 500 μM (**A**,**C**,**D**) and 40 μM (**B**). Black arrows indicate vesiculation of the cytoplasmic membrane.

A comprehensive cell culture micrograph is presented below (Figure 5). The micrograph was obtained by overlaying three images obtained in different fluorescence channels. The nuclei of all the cells before plasma treatment are colored blue on the micrograph (Hoechst 33342, Figure 5A). After plasma treatment, the vast majority of the cells acquired pink-colored nuclei of varying intensities (propidium iodide), indicating that these cells were damaged and were in different stages of apoptosis (Figure 5B).
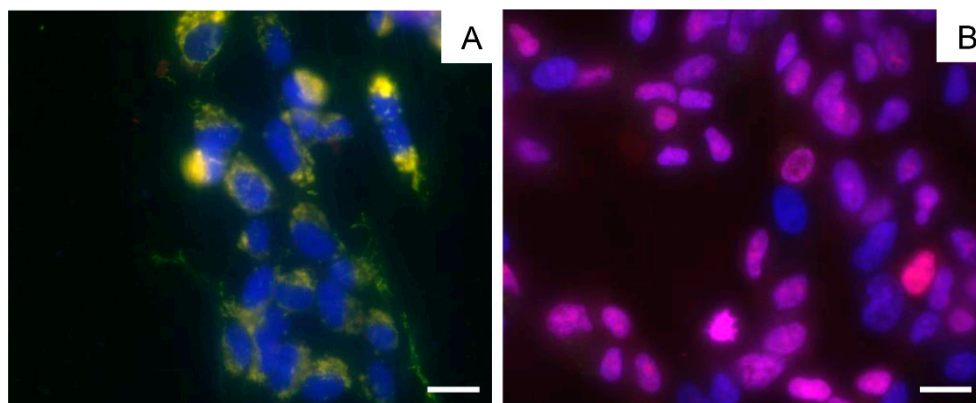

Figure 5. Micrographs of the BMSC culture before plasma treatment (**A**) and 24 h after exposure to LTP (**B**), obtained by an overlay of three fluorescent channels and transmitted light. Cytoplasm is colored green, viable cell nuclei are colored blue (Hoechst 33342) and a pink color (propidium iodide) indicates apoptotic cell nuclei. The scale bars are 20 μM.

We also evaluated the expression level of a gene of one of the key enzymes activated during apoptosis, effector caspase 3, as well as a gene of c-Jun-N-terminal protein kinase (JNK) involved in the initiation of apoptosis, including in response to the development of oxidative stress [34]. As can be seen from Figure 6, the level of gene expression of these apoptosis factors in stem cells increased

significantly during the first two days after exposure to LTP and showed a tendency to decrease on the third day.
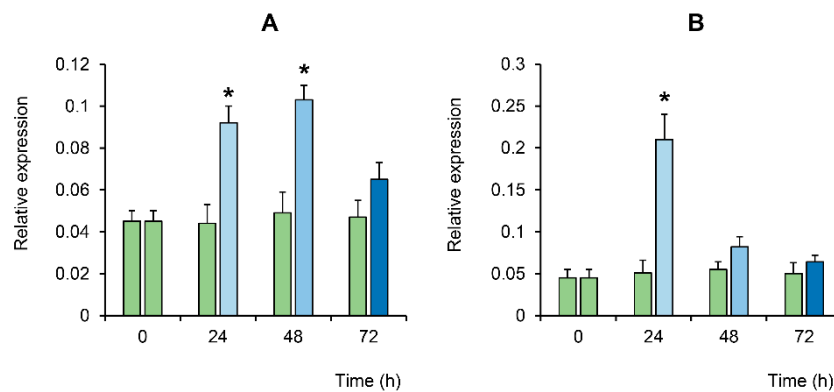
A

B

Figure 6. Changes in the relative expression of caspase 3 (**A**) and JNK (**B**) in the BMSC culture at different times after LTP exposure (relative to bAct, shown by the blue bars). The green bars indicate no exposure to plasma (i.e., the control). The values are given as means ± SEM (*n* = 3). * *p* < 0.05 compared to the control.

It is known that ROS, along with the induction of destructive processes, can also stimulate regenerative processes in the tissues of living organisms [20–22]. One of the mechanisms of inducing cell proliferation is the participation of ROS in the activation of mitogenic signaling pathways [34]. It is known that various growth factors with mitogenic activity, such as platelet-derived growth factor (PDGF), FGFb and epidermal growth factor (EGF), activate mitogen-activated protein (MAP) kinase mitogenic pathways, in which ROS generated by nicotinamide-adenine dinucleotide phosphate (NADPH) oxidase are a necessary component [38]. In this paper, we estimated the effect of LTP on the level of fibroblast growth factor (FGFb) in BMSC. One can see that after exposure to LTP, the level of FGFb showed a time-dependent tendency to increase (Figure 7).
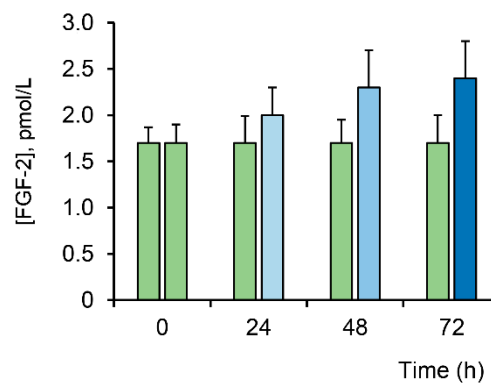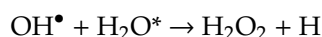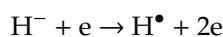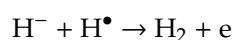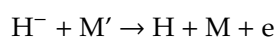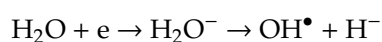

Figure 7. Evaluation of the fibroblast growth factor (FGFb) level in BMSC at different times after LTP exposure (blue bars). Data are represented as the means ± SEM (*n* = 3). The green bars indicate no exposure to plasma.

4. Discussion

It is known that both long-lived (O_3 and H_2O_2) and short-lived ($^{\bullet}OH$ and $O_2^{-\bullet}$) ROS may be produced under various physiological (e.g., the natural process of aging) as well as pathological conditions (e.g., cerebellar ischemia, atherosclerosis and sunburns). The excessive generation of ROS leads to the development of oxidative stress, which causes damage to cells and cell death. However, some reports also indicate the crucial role of ROS in the regulation of the metabolism, proliferation and cell differentiation [20–22].

LTP was found to be accompanied by the formation of various types of ROS exhibiting biological activity. Depending on the concentration, ROS can both damage biological macromolecules and play a significant regulatory role. For example, in the case of tissue rupture, ROS can, on one hand, contribute to the wound's healing process, and, on the other hand, lead to the inactivation of pathogenic microorganisms. It is important to note that these biological effects of LTP were observed mainly in a liquid medium, which indicates that chemically active substances produced by the action of plasma on the gas phase can be transported by diffusion into liquid media. The number of various forms of ROS generated by LTP largely depends on the composition of the liquid medium, the plasma parameters and the exposure time [39].

As established in the present work, a significant amount of hydrogen peroxide was actually formed in the aqueous solution when exposed to LTP (Figure 2A). Plasma was formed by the ionization of water vapor molecules. The most likely ionization mechanism was the dissociation of water molecules through dissociative electron attachment [40], resulting in the formation of negatively charged H_2O^-. The latter is unstable and decomposes into a neutral hydroxyl radical and a negatively charged hydrogen ion. The main reactions in plasma proceed according to the following scheme:

$$H_2O + e \rightarrow H_2O^- \rightarrow OH^\bullet + H^-$$

$$H^- + M' \rightarrow H + M + e$$

$$H^- + H^\bullet \rightarrow H_2 + e$$

$$H^- + e \rightarrow H^\bullet + 2e$$

$$OH^\bullet + H_2O^* \rightarrow H_2O_2 + H$$

In this case, multiple use of one electron occurs, which ensures a chain process in the proceeding reaction.

The acute effect of ROS within 1 h after LTP exposure led to a significant increase in the level of DC and MDA in the BMSC culture (Figure 2B,C), which is evidence of the development of lipid peroxidation of the cell membranes and oxidative stress. In this case, the level of LPO products strongly correlated with the level of H_2O_2 in the medium ($R^2 = 0.96$) and also showed a tendency to decrease to the control values by the third day of incubation. Hence, one could assume that the acute effect of LTP-induced ROS is associated with the development of oxidative processes, including lipid peroxidation of the BMSC membranes.

It is quite obvious that the highest local concentrations of ROS were observed in the plasma exposure zone (near the needle of the electrode). One can suppose that the primary effects of LTP on BMSC are caused by the direct action of plasma through the generation of ions, electrons and short-living ROS, formed at the moment of action of LTP and acting in close proximity of the electrode. Indeed, the addition of long-lived hydrogen peroxide at concentrations generated by LTP treatment (50–100 µM) did not significantly affect the mitochondrial potential of BMSC (Figure 3K,L), nor the cell survival and proliferation (data not shown), which corresponds to data from the literature on the effect of such concentrations of hydrogen peroxide on cell cultures [41]. At the same time, the further effect on BMSC might be related to examples of long-lived ROS (e.g., H_2O_2, which is able to spread across the whole Petri dish via diffusion). Lipid peroxidation and oxidative stress are generally considered as common triggers that initiate the process of cell death [34]. One could assume that mitochondria play a key role in this process. Indeed, it can be seen that the acute action of ROS during the first days after LTP exposure initiates mitochondrial dysfunction, presumably through mitophagy, as evidenced by a decrease in the membrane potential of mitochondria which, most likely, leads to an increase in the expression of PINK1/Parkin and the triggering of the signaling pathway, leading to the formation of autophagosomes and subsequent delivery to lysosomes for complete destruction [42]. This is accompanied by the suppression of mitochondrial biogenesis (decreased expression of PGC-1a), as well as the processes of fusion and fission of the organelles (decreased expression of OPA1, MFN1,

MFN2 and DRP1). Eventually, the BMSC show signs of massive degradation of damaged organelles (increased FIS1 expression and decreased mtDNA/nDNA ratio). Destructive changes are also found at the cellular level. Indeed, as can be seen from the microscopy data (Figures 4 and 5), the BMSC located in the zone of direct action of LTP showed morphological changes specific to apoptosis, manifested in the formation of apoptotic bodies (Figure 4B). The Hoechst 33342/PI dual-staining assay also showed typical apoptotic morphology for the BMSC upon LTP treatment (Figure 5B). The results of real-time PCR analysis confirmed the data obtained and indicated a significant increase in the expression of the protein factors of apoptosis-caspase 3 and JNK during the first hour after LTP exposure (Figure 6). Caspase-3 is a cysteine-aspartic acid executioner protease that is best known for its enzymatic function at the end of the intrinsic apoptotic cascade [43]. Caspase 3 is known to be activated in an apoptotic cell both externally (via death ligands) and intrinsically, primarily due to the release of the cytochrome *c* from mitochondria, induced by mitochondrial dysfunction and the opening of mitochondrial permeability transition (MPT) pores [34,35,44]. In turn, the activation of JNK leads to its translocation into the mitochondrial membrane, where it blocks the anti-apoptotic protein Bcl-2, which contributes to the sequential activation of proapoptotic members of the Bcl-2 family, which are critical for the release of the cytochrome *c* from mitochondria and the induction of apoptosis [34]. Both of these cascades are directly initiated by ROS under the condition of oxidative stress [34]. Hence, one could assume that the initiation of cell death by apoptosis due to the overproduction of ROS and mitochondrial degradation underlies the acute action of LTP, which was observed during the first hour after plasma exposure to the cell culture.

It can be seen that the intensity of oxidative stress due to the LTP-induced hyperproduction of ROS showed a tendency to decrease after reaching its maximum in the first hour after LTP exposure. This was manifested both in the decreased concentration of hydrogen peroxide in the medium and in the lowered concentration of lipid peroxidation products (DC and MDA) in the cell culture. One could assume that this was a consequence of the activation of intracellular antioxidant defense systems that normalize the ROS concentration in the cell [45]. Indeed, we found that the expression of cytosolic antioxidant enzymes SOD 1 (superoxide dismutase 1) and GPX1 (glutathione peroxidase 1) increased 1.8 and 2.2 times, respectively, during the first 24 h after LTP exposure (data not shown). In addition, the expression of the mitochondrial antioxidant protein SOD2 (superoxide dismutase 1) increased almost 6.5 times during this period (data not shown), which most likely contributed to the further restoration of the functional activity of the mitochondria. Indeed, the BMSC display alleviated PINK1/Parkin expression and the intensity of mitochondrial dysfunction, which was accompanied by an increase in the membrane potential of the organelles. It should be noted that there was significant activation of mitochondrial biogenesis (an increase in PGC-1a expression and the mtDNA/nDNA ratio) and the processes of fusion and fission of organelles, which was evidenced by the significantly increased levels of OPA1, MFN and MFN2 involved in the fusion of organelles, as well as by the expression of the FIS1 factor, which also plays an important role in the process of mitochondrial fission [36,38]. In this case, these parameters characterizing mitochondrial biogenesis and dynamics significantly exceeded the parameters of the cells before LTP treatment. An increase in the intensity of these processes at the mitochondrial level also seemed to contribute to the time-dependent stimulation of proliferation and differentiation of the stem cells. Indeed, as shown in this work, the effect of LTP on human BMSC was also accompanied by the activation of proliferative processes, as evidenced by a tendency to increase the level of the FGFb in the BMSC in response to LTP (Figure 7). It was previously shown that LTP has a similar time- or dose-dependent effect on the growth and differentiation of various mammalian cell lines [20–22].

5. Conclusions

The obtained preliminary results indicate the important role of mitochondria in the formation of the cellular response to LTP exposure. Indeed, it seems that LTP can initiate destructive processes leading to mitochondrial dysfunction and cell death, as well as stimulating mitochondrial biogenesis,

which promotes cell proliferation. A thorough study of this phenomenon and, in particular, the effect of LTP on cell differentiation is required in order to assess the prospects of using plasma in regenerative medicine.

References

1. Weltmann, K.D.; Kindel, E.; Woedtke, T.; Hähnel, M.; Stieber, M.; Brandenburg, R. Atmospheric-pressure plasma sources: Prospective tools for plasma medicine. *Pure Appl. Chem.* **2010**, *82*, 1223–1237. [CrossRef]

2. Yousfi, M.; Merbahi, N.; Pathak, A.; Eichwald, O. Low-temperature plasmas at atmospheric pressure: Toward new pharmaceutical treatments in medicine. *Fundam. Clin. Pharmacol.* **2014**, *28*, 123–135. [CrossRef] [PubMed]

3. Machala, Z.; Tarabova, B.; Hensel, K.; Spetlikova, E.; Sikurova, L.; Lukes, P. Formation of ROS and RNS in water electro-sprayed through transient spark discharge in air and their bactericidal effects. *Plasma Process. Polym.* **2013**, *10*, 649–659. [CrossRef]

4. Girard, F.; Peret, M.; Dumont, N.; Badets, V.; Blanc, S.; Gazeli, K.; Noël, C.; Belmonte, T.; Marlin, L.; Cambus, J.-P.; et al. Correlations between gaseous and liquid phase chemistries induced by cold atmospheric plasmas in a physiological buffer. *Phys. Chem. Chem. Phys.* **2018**, *20*, 9198–9210. [CrossRef] [PubMed]

5. Burlica, R.; Kirkpatrick, M.J.; Locke, B.R. Formation of reactive species in gliding arc discharges with liquid water. *J. Electrost.* **2006**, *64*, 35–43. [CrossRef]

6. Shapira, Y.; Bormashenko, E.; Drori, E. Pre-germination plasma treatment of seeds does not alter cotyledon DNA structure, nor phenotype and phenology of tomato and pepper plants. *Biochem. Biophys. Res. Commun.* **2019**, *519*, 512–517. [CrossRef]

7. Ziuzina, D.; Boehm, D.; Patil, S.; Cullen, P.J.; Bourke, P. Cold plasma inactivation of bacterial biofilms and reduction of quorum sensing regulated virulence factors. *PLoS ONE* **2015**, *10*, e0138209. [CrossRef]

8. Zhang, Y.; Xiong, Y.; Xie, P.; Ao, X.; Zheng, Z.; Dong, X.; Li, H.; Yu, Q.; Zhu, Z.; Chen, M.; et al. Non-thermal plasma reduces periodontitis-induced alveolar bone loss in rats. *Biochem. Biophys. Res. Commun.* **2018**, *503*, 2040–2046. [CrossRef]

9. Trebulová, K.; Krčma, F.; Kozáková, Z.; Matoušková, P. Impact of microwave plasma torch on the yeast *Candida glabrata*. *Appl. Sci.* **2020**, *10*, 5538. [CrossRef]

10. Schnabel, U.; Yarova, K.; Zessin, B.; Stachowiak, J.; Ehlbeck, J. The combination of plasma-processed air (PPA) and plasma-treated water (PTW) causes synergistic inactivation of *Candida albicans* SC5314. *Appl. Sci.* **2020**, *10*, 3303. [CrossRef]

11. Arndt, S.; Unger, P.; Wacker, E.; Shimizu, T.; Heinlin, J.; Li, Y.F.; Thomas, H.M.; Morfill, G.E.; Zimmermann, J.L.; Bosserhoff, A.K.; et al. Cold atmospheric plasma (CAP) changes gene expression of key molecules of the wound healing machinery and improves wound healing in vitro and in vivo. *PLoS ONE* **2013**, *8*, e79325. [CrossRef] [PubMed]

12. Cui, H.S.; Joo, S.Y.; Cho, Y.S.; Park, J.H.; Kim, J.-B.; Seo, C.H. Effect of Combining Low Temperature Plasma, Negative Pressure Wound Therapy, and Bone Marrow Mesenchymal Stem Cells on an Acute Skin Wound Healing Mouse Model. *Int. J. Mol. Sci.* **2020**, *21*, 3675. [CrossRef] [PubMed]

13. Ponte, G.D.; Sardella, E.; Fanelli, F.; d'Agostino, R.; Favia, P. Trends in surface engineering of biomaterials: Atmospheric pressure plasma deposition of coatings for biomedical applications. *Eur. Phys. J. Appl. Phys.* **2011**, *56*, 24023. [CrossRef]

14. Canal, C.; Modic, M.; Cvelbar, U.; Ginebra, M.P. Regulating the antibiotic drug release from β-tricalcium phosphate ceramics by atmospheric plasma surface engineering. *Biomater. Sci.* **2016**, *4*, 1454. [CrossRef] [PubMed]

15. Kwon, J.-S.; Kim, Y.H.; Choi, E.H.; Kim, K.-N. The effects of non-thermal atmospheric pressure plasma jet on attachment of osteoblast. *Curr. Appl. Phys.* **2013**, *13*, S42. [CrossRef]

16. Metelmann, P.H.; Nedrelow, D.S.; Schuster, M.; Rutkowski, R.; Seebauer, C. Clinical studies applying physical plasma in head and neck cancer-key points and study design. *Int. J. Clin. Res. Trials* **2016**, *1*, 103. [CrossRef]

17. Panngom, K.; Baik, K.Y.; Ryu, Y.H.; Uhm, H.S.; Choi, E.H. Differential responses of cancer cell lines to non-thermal plasma from dielectric barrier discharge. *Curr. Appl. Phys.* **2013**, *13*, S6. [CrossRef]

18. Jo, A.; Joh, H.M.; Chung, J.W.; Chung, T.H. Cell viability and measurement of reactive species in gas- and liquid-phase exposed by a microwave-excited atmospheric pressure argon plasma jet. *Curr. Appl. Phys.* **2020**, *20*, 562. [CrossRef]

19. Kalghatgi, S.; Kelly, C.M.; Cerchar, E.; Torabi, B.; Alekseev, O.; Fridman, A.; Friedman, G.; Azizkhan-Clifford, J. Effects of non-thermal plasma on mammalian cells. *PLoS ONE* **2011**, *6*, e16270. [CrossRef]

20. Xu, D.; Luo, X.; Xu, Y.; Cui, Q.; Yang, Y.; Liu, D.; Chen, H.; Kong, M.G. The effects of cold atmospheric plasma on cell adhesion, differentiation, migration, apoptosis and drug sensitivity of multiple myeloma. *Biochem. Biophys. Res. Commun.* **2016**, *473*, 1125. [CrossRef]

21. Liu, J.; Xu, G.; Shi, X.; Zhang, G.-J. Low temperature plasma promoting fibroblast proliferation by activating the NF-κB pathway and increasing cyclinD1 expression. *Sci. Rep.* **2017**, *7*, 11698. [CrossRef] [PubMed]

22. Tominami, K.; Kanetaka, H.; Sasaki, S.; Mokudai, T.; Kaneko, T.; Niwano, Y. Cold atmospheric plasma enhances osteoblast differentiation. *PLoS ONE* **2017**, *12*, e0180507. [CrossRef]

23. Ashurov, M.K.; Belov, S.V.; Gudkov, S.V.; Danyleiko, Y.K.; Egorov, A.B.; Savranskii, V.V.; Temnov, A.A. Effects of low-temperature plasma glow discharge on the proliferative activity of cells and the repair functions of tissues in animals and plants. *Biomed. Eng.* **2020**, *53*, 407–412. [CrossRef]

24. Belosludtsev, K.N.; Dubinin, M.V.; Belosludtseva, N.V.; Mironova, G.D. Mitochondrial Ca^{2+} transport: Mechanisms, molecular structures, and role in cells. *Biochemistry* **2019**, *84*, 593–607. [CrossRef]

25. Baburin, N.V.; Belov, S.V.; Danileiko, Y.K.; Egorov, A.B.; Lebedeva, T.P.; Nefedov, S.M.; Osiko, V.V.; Salyuk, V.A. Heterogeneous recombination in steam plasma as a mechanism of affecting biological tissues. *Dokl. Phys.* **2009**, *54*, 259. [CrossRef]

26. Cherrington, B.E. *Gaseous Electronics and Gas Laser*; Pergamon Press: Oxford, UK, 1982.

27. Gudkov, S.V.; Guryev, E.L.; Gapeyev, A.B.; Sharapov, M.G.; Bunkin, N.F.; Shkirin, A.V.; Zabelina, T.S.; Glinushkin, A.P.; Sevost'yanov, M.A.; Belosludtsev, K.N.; et al. Unmodified hydrated C60 fullerene molecules exhibit antioxidant properties, prevent damage to DNA and proteins induced by reactive oxygen species and protect mice against injuries caused by radiation-induced oxidative stress. *Nanomed. Nanotechnol. Biol. Med.* **2019**, *15*, 37.

28. Moore, K.; Roberts, L.J. Measurement of lipid peroxidation. *Free Radic. Res.* **1998**, *28*, 659. [CrossRef]

29. Hodges, D.M.; DeLong, J.M.; Forney, C.F.; Prange, R.K. Improving the thiobarbituric acid-reactive-substances assay for estimating lipid peroxidation in plant tissues containing anthocyanin and other interfering compounds. *Planta* **1999**, *207*, 604. [CrossRef]

30. Scaduto, R.C., Jr.; Grotyohann, L.W. Measurement of mitochondrial membrane potential using fluorescent rhodamine derivatives. *Biophys. J.* **1999**, *76*, 469–477. [CrossRef]

31. Ye, J.; Coulouris, G.; Zaretskaya, I.; Cutcutache, I.; Rozen, S.; Madden, T. Primer-BLAST: A tool to design target-specific primers for polymerase chain reaction. *BMC Bioinform.* **2012**, *13*, 134. [CrossRef]

32. Sharapov, M.G.; Novoselov, V.I.; Penkov, N.V.; Fesenko, E.E.; Vedunova, M.V.; Bruskov, V.I.; Gudkov, S.V. Protective and adaptogenic role of peroxiredoxin 2 (Prx2) in neutralization of oxidative stress induced by ionizing radiation. *Free Radic. Biol. Med.* **2019**, *134*, 76. [CrossRef]

33. Quiros, P.M.; Goyal, A.; Jha, P.; Auwerx, J. Analysis of mtDNA/nDNA Ratio in Mice. *Curr. Protoc. Mouse Biol.* **2017**, *7*, 47–54. [CrossRef]

34. Su, L.J.; Zhang, J.H.; Gomez, H.; Murugan, R.; Hong, X.; Xu, D.; Jiang, F.; Peng, Z.-Y. Reactive oxygen species-induced lipid peroxidation in apoptosis, autophagy, and ferroptosis. *Oxidative Med. Cell Longev.* **2019**, *2019*, 5080843. [CrossRef]

35. Xiao, M.; Zhong, H.; Xia, L.; Tao, Y.; Yin, H. Pathophysiology of mitochondrial lipid oxidation: Role of 4-hydroxynonenal (4-HNE) and other bioactive lipids in mitochondria. *Free Radic. Biol. Med.* **2017**, *111*, 316–327. [CrossRef]

36. Fu, W.; Liu, Y.; Yin, H. Mitochondrial Dynamics: Biogenesis, Fission, Fusion, and Mitophagy in the Regulation of Stem Cell Behaviors. *Stem Cells Int.* **2019**, *2019*, 9757201. [CrossRef]

37. Yang, X.; Pan, W.; Xu, G.; Chen, L. Mitophagy: A crucial modulator in the pathogenesis of chronic diseases. *Clin. Chim. Acta* **2020**, *502*, 245–254. [CrossRef]

38. Gomes, L.C.; Scorrano, L. High levels of Fis1, a pro-fission mitochondrial protein, trigger autophagy. *Biochim. Biophys. Acta* **2008**, *1777*, 860–866. [CrossRef]

39. Takamatsu, T.; Uehara, K.; Sasaki, Y.; Miyahara, H.; Matsumura, Y.; Iwasawa, A.; Ito, N.; Azuma, T.; Kohno, M.; Okino, A. Investigation of reactive species using various gas plasmas. *RSC Adv.* **2014**, *4*, 39901. [CrossRef]

40. Rusanov, V.D.; Fridman, A.A.; Sholin, G.V. The physics of a chemically active plasma with nonequilibrium vibrational excitation of molecules. *Sov. Phys. Uspekhi* **2014**, *24*, 447–474. [CrossRef]

41. Sies, H. Findings in redox biology: From H_2O_2 to oxidative stress. *J. Biol. Chem.* **2020**, *295*, 13458–13473. [CrossRef] [PubMed]

42. Bakula, D.; Scheibye-Knudsen, M. MitophAging: Mitophagy in Aging and Disease. *Front. Cell Dev. Biol.* **2020**, *8*, 239. [CrossRef] [PubMed]

43. Liu, J.; Wang, F.; Yin, D.; Zhang, H.; Feng, F. Caspase 3 may participate in the anti-tumor immunity of dendritic cells. *Biochem. Biophys. Res. Commun.* **2019**, *511*, 447. [CrossRef] [PubMed]

44. Belosludtsev, K.N.; Belosludtseva, N.V.; Dubinin, M.V. Diabetes mellitus, mitochondrial dysfunction and Ca^{2+}-dependent permeability transition pore. *Int. J. Mol. Sci.* **2020**, *21*, 6559. [CrossRef] [PubMed]

45. Halliwell, B.; Gutteridge, J. *Free Radicals in Biology and Medicine*, 4th ed.; Oxford University Press: New York, NY, USA, 2007.